International Journal of Solids and Structures 49 (2012) 3316–3322

Contents lists available at SciVerse ScienceDirect

International Journal of Solids and Structures

journal homepage: www.elsevier.com/locate/ijsolstr

2D and 3D finite element analysis of crack growth under compressive residual stress field

M.H. Gozin, M. Aghaie-Khafri *

Faculty of Mechanical Engineering, K.N. Toosi University of Technology, 1999-143344 Tehran, Iran

ARTICLE INFO

Article history:
Received 11 February 2012
Received in revised form 8 May 2012
Available online 31 July 2012

Keywords:
Crack
Fatigue
Finite element
Residual stress

ABSTRACT

In the present study, plasticity induced crack closure (PICC) concept and three dimensional (3D) finite element method (FEM) were used to study the effect of compressive residual stress field on the fatigue crack growth from a hole. Furthermore, a new methodology on the basis of a correction factor was presented to increase the PICC precision. The result obtained was compared to two dimensional (2D) FEM, superposition method and Liu's experimental data. To simulate the elasto-plastic behavior of the material, isotropic hardening was assumed and the Von-Mises yield criterion was implemented. A 3D mesh was built using eight-node hexahedral elements and one half of the specimen was modeled. The simulation results were fairly well correlated with experimental data. Furthermore, the 3D elasto-plastic FEM predicted a slightly smaller fatigue life than a 2D plane stress FEM. Applying the modified PICC method reduces the 3D FEM fatigue life prediction errors.

1. Introduction

The effect of residual stress on the fatigue crack propagation is of great practical significance and has, therefore, been the focus of much research. Considering the reliability and operational life of components containing residual stress, it is important to determine the fatigue crack growth under residual stress field. The effect of residual stress on fatigue crack growth has been extensively studied based on the superposition techniques due to their simplicity. In superposition-based techniques, the stresses due to an applied mechanical load are assumed to superimpose linearly on the residual stress.

The usage of the superposition has been criticized in view of the fact that it only considers the initial residual stress field that exists in the uncracked structure. The redistribution of the residual stress while the propagating fatigue crack penetrates the residual stress field is neglected. Moreover, it has been pointed out that superposition is invalid while the crack faces contact (Jones and Dunn, 2009; Parker, 1982).

The PICC concept suggested by Elber (1970) has been supported by many investigations. It can be used to incorporate crack shielding mechanisms into fatigue crack growth rate models. During fatigue process, PICC occurs due to that the yielded material left in the wake of a crack tip as it propagates through plastic zones. The plastic wake enables the crack to close before minimum load is reached. Elber (1970) showed that the stress intensity factor at the crack tip does not change while the crack is closed.

Roughness-induced crack closure, oxide-induced crack closure, fluid pressure-induced crack closure and phase transformation-induced crack closure are used to account crack closure (Castro and Potirniche, 2010). However, finite element modeling based on PICC concept has been concerned by many researchers (Solanki et al., 2004; McClung and Sehitoglu, 1989; Zhang and Bowen, 1998; Ismonov and Daniewicz, 2010; Sheu et al., 1995; De Matos and Nowel, 2007). A basic algorithm was employed by many researchers. An elasto-plastic finite element model is built with a suitably refined mesh; then, time-dependent remote tractions are applied to simulate cyclic loading. The crack tip node is released during each cycle and the crack tip is extended one element length per cycle. Consequently, a plastic wake will be formed. Crack closure is predicted by monitoring the contact between crack faces. This process is repeated until the crack opening stress values have been stabilized. A detailed discussion is given by Skinner and Daniewicz (2001).

Fatigue crack growth from a central hole in a sheet, preyielded by a remote tensile load has been used as an example where superposition predictions do not correlate well with experimental data (LaRue and Daniewicz, 2007). Liu (1979) originally measured fatigue crack growth rates from preyielded holes in aluminum AA2024-T351 sheets. Liu noted that crack growth in the residual stress fields of the preyielded holes was faster than baseline fatigue crack growth at higher applied ΔK levels (LaRue and Daniewicz, 2007). This was unexpected because Liu (1979) KR solutions were

* Corresponding author. Tel.: +98 09123088389; fax: +98 21 886 74748.
E-mail address: maghaei@kntu.ac.ir (M. Aghaie-Khafri).

0020-7683/$ - see front matter
http://dx.doi.org/10.1016/j.ijsolstr.2012.07.014

negative over the entire range of crack length, and therefore should only have slowed crack growth compared to the baseline data.

Newman (1981) modified FASTRAN to predict crack growth rates through initial residual stress fields and analyzed Liu's fatigue experiments. FASTRAN is based upon a Dugdale (1960) strip yield model that is modified to include plastic deformation at the crack front and in the crack wake. Since FASTRAN models plastic deformation, changes to residual stress due to changes in the plastic strain field during fatigue should be naturally captured. Residual stress was introduced into FASTRAN by overloading a crack, leaving a residual stress field simulating the residual stress surrounding a preyielded hole. FASTRAN life predictions correlated well with Liu (1979) data, within a factor of 1.2.

LaRue and Daniewicz (2007) analyzed Liu's experiments with a ΔK_{eff} approach, but used 2D elasto–plastic finite element analysis of the actual cracked specimen under repeated loading and unloading to solve for K_{open}. The ΔK_{eff} life predictions again correlated well with Liu (1979) data, within a factor of 1.2. LaRue and Daniewicz (2007) also predicted fatigue life using superposition. The superposition prediction correlated poorly with Liu (1979) life data, over-predicting life by a factor of approximately 2.5. However, they did not discuss why the ΔK_{eff} prediction differed so greatly from the superposition prediction.

Jones and Dunn (2009) predicted fatigue experiments of Liu (1979) using linear elastic fracture mechanics and the principle of superposition. They concluded that a 3D elasto–plastic finite element model predicted a slightly smaller compressive residual stress than a 2D plane stress finite element model. Yet, the two residual stress distributions resulted in predicted fatigue lives that differed by a factor of 2. This highlights the sensitivity of fatigue life to the initial residual stresses. Changing the initial crack size in the fatigue prediction from 2 to 2.83 mm, to allow for the minimum pre-crack required by ASTM-E647, caused the predicted life to be reduced by a factor as large as 2.3. This highlights the sensitivity of fatigue life to initial crack size.

A relatively small number of investigators have modeled PICC in 3D geometries using FEM (Chermahini and Blom, 1991; Skinner and Daniewicz, 2001; Chermahini and Blom, 1993; Seshadri, 1995; Solanki, 2002). In a 3D geometry, the crack opening value will vary along the crack front. This variation will result in different portions of the crack front growing with different rates under the cyclic loading. Consequently, the crack front shape will naturally evolve. This crack shape evolution makes modeling of 3D geometries much more complex. For simplicity this shape evolution is generally neglected and the crack front is extended uniformly.

The purpose of this study is to determine the sensitivity of PICC method to initial residual stress field and the effect of initial crack size on the fatigue life prediction. A 3D finite element analysis of preyielded hole was developed and the results obtained were compared with Liu (1979) experimental data.

2. Material, specimens and tests

The starting material used by Liu (1979) experiments was AA2024-T351. Liu (1979) measured fatigue crack growth from a hole using the specimen shown in Fig. 1. The bilinear stress–strain curve of this material is shown in Fig. 2. Center-cracked specimens were also tested under constant amplitude cyclic loading to develop baseline crack growth rate (da/dN) curves at R values of 0.1 and 0.7. Jones and Dunn (2009) modified Liu (1979) crack growth results using Harter method to cover more stress ratios. Liu (1979) preyielded hole fatigue experiments were conducted using $305 \times 76 \times 6.35$ mm aluminum AA2024-T351 specimens with centrally located 19 mm diameter holes. A remote 250 MPa tensile uniform stress was applied and removed, resulting in residual stress near the hole. A 0.152 mm wide electrical discharge machining (EDM) slot was cut into one side of the hole. The specimens were then cycled to produce a notch plus pre-crack length of approximately 2 mm. One specimen, A2-30, was then fatigued with R = 0.1 and P_{max} = 103 MPa constant amplitude cyclic loading. Three other specimens, A2-19, A2-20, and A2-31, were fatigued at a higher P_{max} = 124 MPa stress level. In the present study just the A2-30 is analyzed.

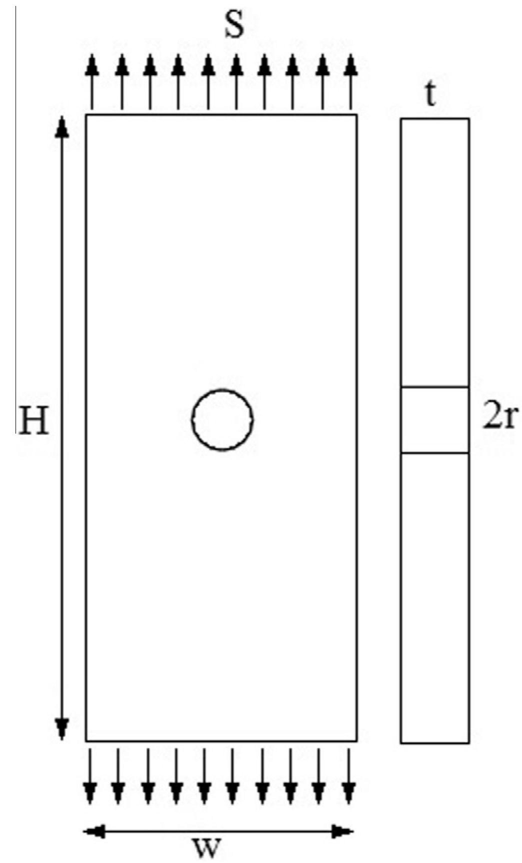

Fig. 1. Fatigue crack growth specimen.

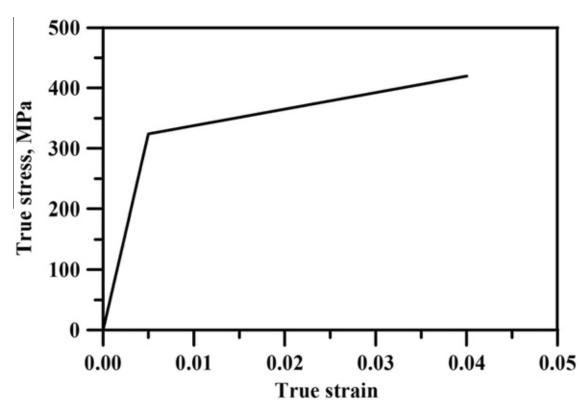

Fig. 2. Bilinear stress–strain curve for AA2024.

3. Finite element simulation

3.1. Residual stress

3.1.1. 2D FEM

The residual stress was analyzed using a one-quarter symmetry 2D plane stress elasto–plastic finite element model. The model composed of 4-noded isoparametric quadrilateral elements with reduced order integration. The commercial finite element program ABAQUS 6.8.1 was used. A bilinear stress–strain curve (Fig. 2) was used to represent the material behavior. The isotropic hardening model is used in the present investigation. However, AA2024-T351 also exhibits kinematic hardening. The kinematic hardening changes the plastic deformed areas both ahead and behind the crack tip. This affects the residual stress field ahead of the crack tip. Consequently, the crack propagation life will be decreased. In the present study neglecting the kinematic hardening would cause the predictions slightly overestimate the fatigue life of specimens. The finite element analysis consisted of applying the overload stress and then removing it. The mesh density was progressively doubled until the predicted residual stress along the horizontal axis near the hole converged to within 1.15 MPa at minimum element size of 0.05 mm.

3.1.2. 3D FEM

The overloading was also modeled in 3D with a one-quarter symmetry finite element model using 8-noded hexahedral elements. The planar mesh density of elements was set the same as 2D FEM. Mesh density through the half-thickness was increased to 31 upon which the residual stresses along the future crack line converged to 1.6 MPa. The overload caused significant plastic flow near the hole edges that resulted in residual stresses near the compressive yield strength.

The residual stress generated in 2D models is nearly the same as 3D model at edge nodes as it is shown in Fig. 3. This is a result of the fact that the plane stress condition was assumed in 2D analyses. However, the observed difference between 2D and 3D results at mid-thickness nodes confirmed that the specimen is not ideally at plane stress condition.

3.2. Fatigue crack growth

3.2.1. 3D FEM

Fatigue crack growth from a hole with a pre-existing compressive residual stress is simulated using a 3D elasto–plastic finite element analyses. To simulate the stress–strain behavior of the material, bilinear elastic–plastic model was chosen and the Von-Mises yield criterion was implemented. A 3D mesh was built using eight nodes hexahedral stress elements. Concerning specimen symmetry, one half of the sample was modeled. Mesh refinement procedure was used around the crack tip region to approach predefined convergence. The final mesh consisted of 40856 elements and 45245 nodes (Fig. 4). The elements along the direction of crack advance had a length of 0.05 mm. There are 30 elements through part thickness. To simulate the overload and induce the residual stress, a uniform remote stress of 250 MPa was applied and removed. To simulate the slotting process, elements near the hole's surface with dimension equal to the slot width of 0.152 mm were removed from the mesh using the model change command in ABAQUS. Following the residual stress and the slotting simulation, fatigue crack growth was modeled by repeatedly loading, unloading, advancing the crack (from the slot) and then loading again. The crack was assumed to initiate quickly from the slot, such that no crack incubation period was considered in the analysis. A rigid plate in the plane of crack tip was considered and a frictionless contact between crack faces and rigid plate defined to prevent crack faces penetration. For simplicity the crack shape evolution is neglected and the crack front is extended uniformly.

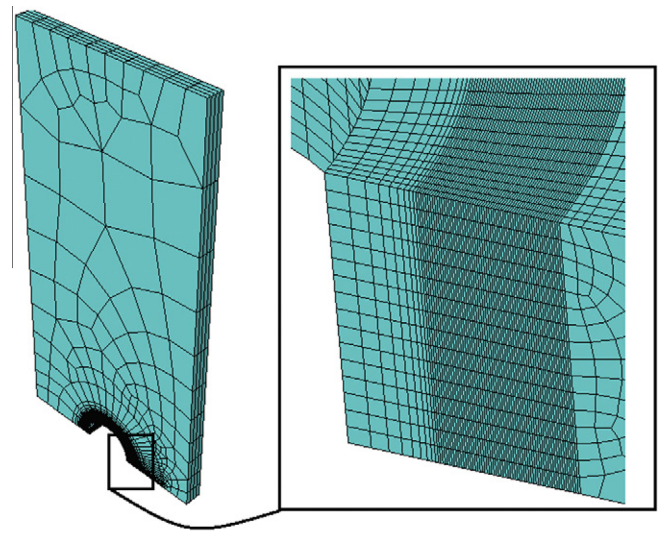

Fig. 4. 3D FEM model and mesh around crack tip zone.

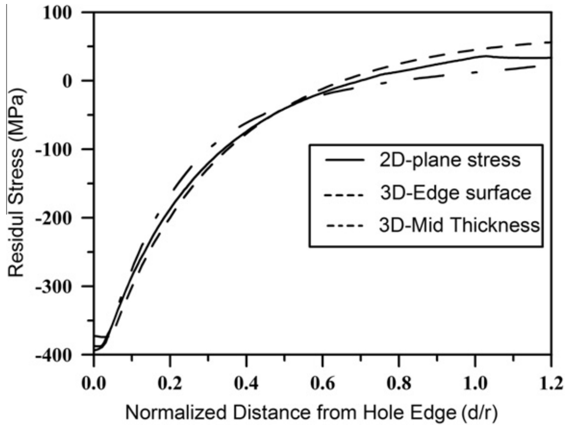

Fig. 3. 2D and 3D FEM residual stress distribution.

3.2.2. 2D FEM

The same method was used for 2D analysis and mesh around crack tip assumed the same as one face of the 3D model.

3.3. Loading sequence

Loading sequence was conducted according to Liu (1979) experiments. The results obtained were compared with experimental data and conventional superposition method.

4. Fatigue crack growth prediction

Considering PICC concept suggested by Elber (1970), effective stress intensity factor is calculated as following:

$$\Delta K_{eff} = K_{max} - K_{op} \quad (1)$$

where K_{max} and K_{op} are the maximum and opening stress intensity factors, respectively. Crack growth rate relates to the effective stress intensity factor by the following equation:

$$\frac{da}{dN} = C(\Delta K_{eff})^m \quad (2)$$

where, c and m are Paris law's coefficients for base material and could be determine by simple CT fatigue crack growth tests. This method consists of calculating crack opening stress from finite element model at each crack length. Then, effective stress intensity factor is determined using Eq. (1). Solving Eq. (2) for dN, results in:

Table 1
Variation of plastic zone size (middle of thickness) with mesh refinement.

Element size (mm)	Number of element at forward plastic zone	Number of element at reversed plastic zone
0.05	30	4
0.1	19	2
0.2	10	1

$$dN = \frac{da}{C(\Delta K_{eff})^m} \quad (3)$$

In a 3D geometry, the crack opening value will vary along the crack front. This variation will result in different portions of the crack front growing with different rates under the cyclic loading. Consequently, the crack front shape will naturally evolve. This crack shape evolution makes modeling of the 3D geometries much more complex. For simplicity's sake, this shape evolution is neglected and the crack front is extended uniformly during the finite element analysis. Then, in each step the opening stress intensity factor would be averaged over the part thickness as following:

$$(K_{opm})_i = \frac{\sum_{j=1}^{f}(K_{opm})_i}{f} \quad (4)$$

where the *i* index denotes for step number and *f* is the number of nodes along crack tip. Inserting K_{opm} into Eq. (1) and then integrating Eq. (3):

$$N_{ai-af} = \sum_{ai}^{af} \frac{a_i}{C(K_{max} - K_{opm})_i^m} \quad (5)$$

The coefficients of Paris's law were calculated on the basis of the Liu (1979) experiment and the interpolation technique. Considering the crack closure method, the crack assumes to be closed under Kop values. Thus, R ratio should be changed in a manner that the crack was closed at lower loads. In the present study the base material crack growth data was considered at different stress ratios. At each crack length, the stress ratio calculated as following:

$$R = \frac{K_{opm}}{K_{max}} \quad (6)$$

Then, for a given crack length the data presented by Liu (1979) experiment was interpolated at the stress ratio of *R*. Finally, the crack growth rate was directly calculated.

5. Results and discussion

5.1. Finite element optimization

Two different types of crack tip plastic zones are generated due to fatigue crack propagation. The first is forward plastic zone which is the plastically deformed material near the crack tip undergoing the maximum load. The second zone of interest is the reversed plastic zone, which is defined as the material near the crack tip undergoing compressive yielding at the minimum load (Solanki et al., 2004).

The variation in the number of elements in the plastic zones as the mesh is refined is listed in Table 1. It is clear that the number of yielded element at the specimen edge is more than the yielded element at the middle of thickness. This is due to the plane stress condition at the edges and approaching to the condition of the plane strain at the middle of the part thickness (Fig. 5). In the present study, mesh density was adjusted based on the number of yielded elements at the middle of thickness to obtain more accurate results. Then, element size was kept constant along the thickness of the model.

5.2. Crack opening stress intensity factor

The effect of a compressive residual stress on the crack opening load was studied following the appropriate mesh refinement and applying adequate number of steps. The results obtained by two and three dimensional finite element crack growth analyses are shown in Figs. 6 and 7, respectively. It can be observed that the opening stresses under the condition of residual stress exhibit a sharp increase up to a normalized crack length of 0.5 and then gradually increases by a moderate slope. The initial sharp increase indicates that the crack growth is slowdown due to the residual stress at the edge of the notch.

The opening stress stabilized at the same distance from the hole edge for both specimens with or without residual stress. Usually, the opening stresses stabilize once the crack tip has passed the

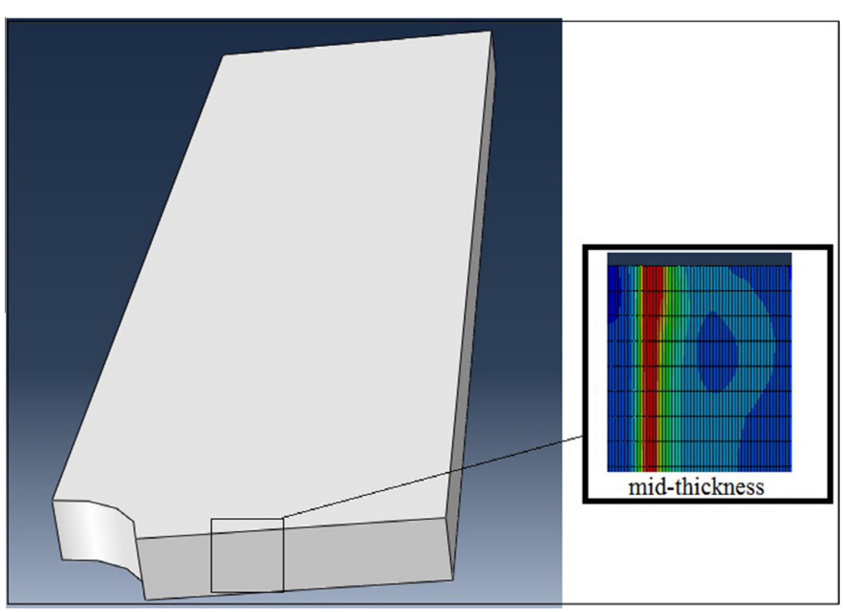

Fig. 5. Crack tip plastic deformation zone.

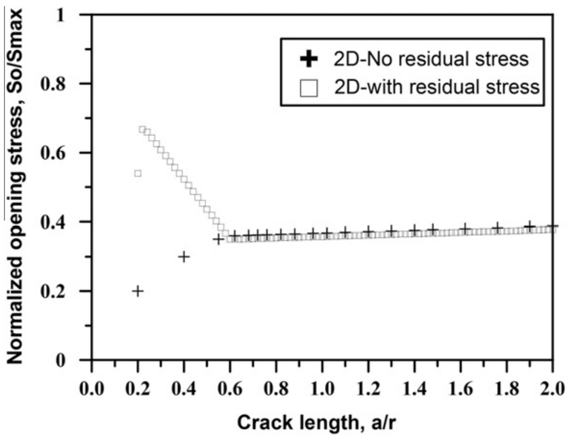

Fig. 6. Normalized crack opening stress intensity factor resulted from 2D FEM.

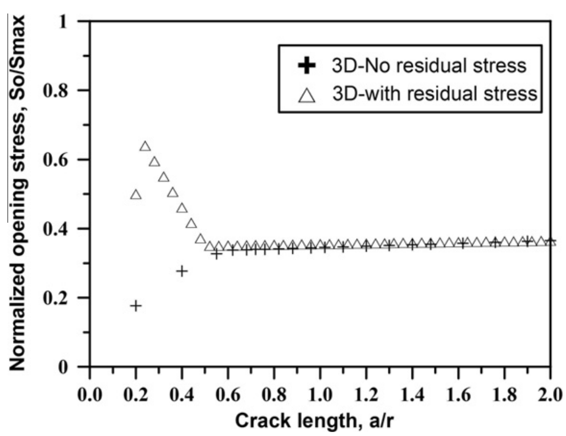

Fig. 7. Avereged crack opening stress intensity factor resulted from 3D FEM.

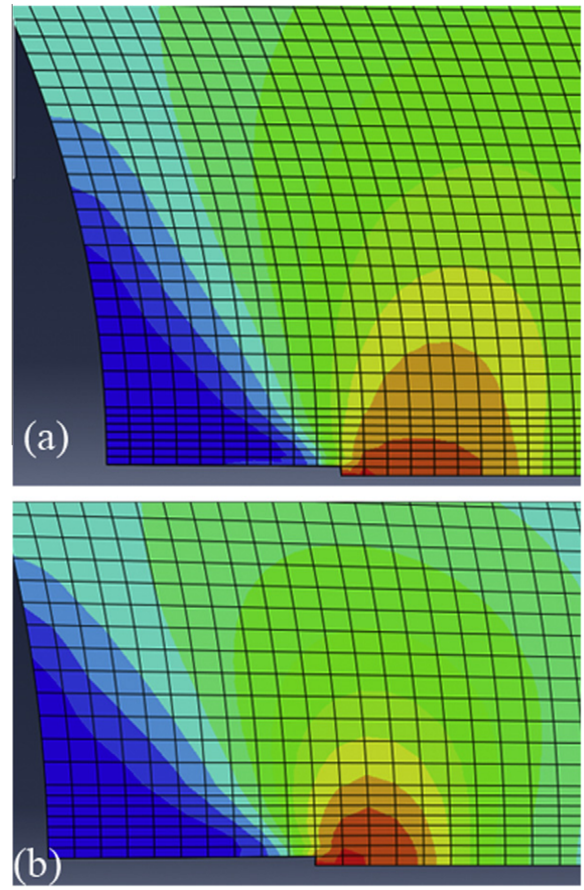

Fig. 8. Crack tip plastic zone following slotting process at (a) without residual stress and (b) with residual stress.

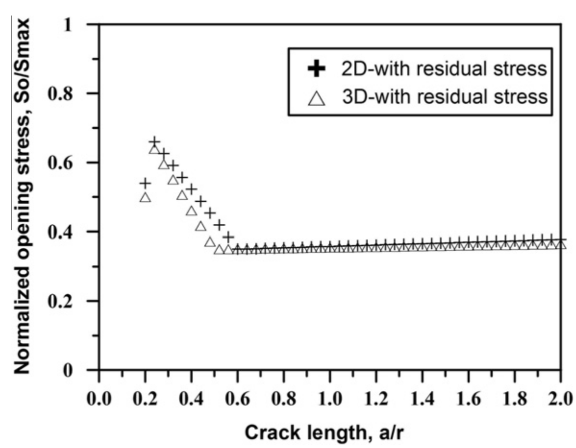

Fig. 9. Normalaized crack opening stress resulted from 2D and 3D FEM.

initial crack tip plastic zone. It should be considered that in the Liu (1979) experiment A2-30 specimen was cut approximately 2 mm following applying a single overload of 250 MPa. Thus, the plastic zone size is decreased by 2 mm. The present analysis considers the slotting by omitting elements in that region. Following this slotting the remained plastic zone size of compressive residual stress is approximately equal to the plastic zone size of no residual stress sequence (Fig. 8). Moreover, it can be considered that the slotting process highly reduces the effect of overload.

The average crack opening stress intensity factors (K_{opm}) at crack tip nodes based on 2D and 3D finite element analysis are shown in Fig. 9. It can be observed that the 2D FEM analysis results in higher opening loads which indicate more intense fatigue crack retardation. This can be related to the plane stress condition assumed in the 2D finite element model.

5.3. Fatigue life prediction

Concerning material properties and Eqs. (1)–(6) the crack growth rates at different effective stress intensity factors were calculated and plotted in Fig. 10. Fatigue life predictions based on the 2D and 3D FEM simulation are compared to Liu (1979) experimental data for A2-30 specimens, shown in Fig. 11. The predicted lives based on the 2D and 3D FEM simulation are differ by a factor of 1.1. It is worth noting that there was also a slight difference in residual stress distribution predicted by the 2D plane stress FEM and the 3D FEM at the middle of thickness, shown in Fig. 3. The slight difference between 2D and 3D FEM predictions indicates that the plane stress condition hypothesis is suitable and does not alter the results accuracy.

Concerning 2D and 3D FEM predictions (Fig. 11), 2D FEM results are in better agreement with Liu's experiments. This is a result of that the PICC was assumed to be the dominant mechanism of crack closure and the effects of other crack closure mechanisms were neglected. This assumption results in conservative predictions of K_{op} and fatigue life. It is interesting to note that the 2D FEM analysis overestimates the opening stress intensity factor. Thus, the errors arise due to the neglecting other mechanisms of crack closure are decreased. Furthermore, the difference between fatigue life

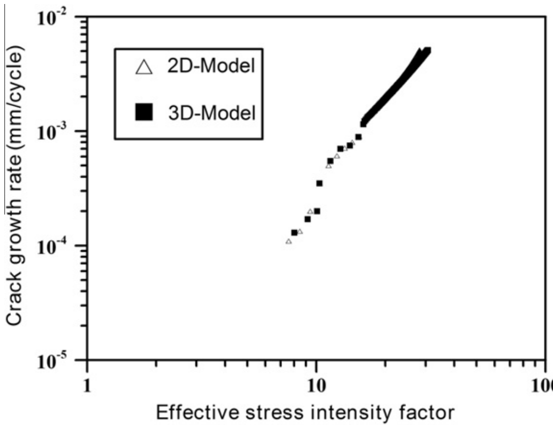

Fig. 10. Variation of predicted crack growth versus effective stress intesity factor.

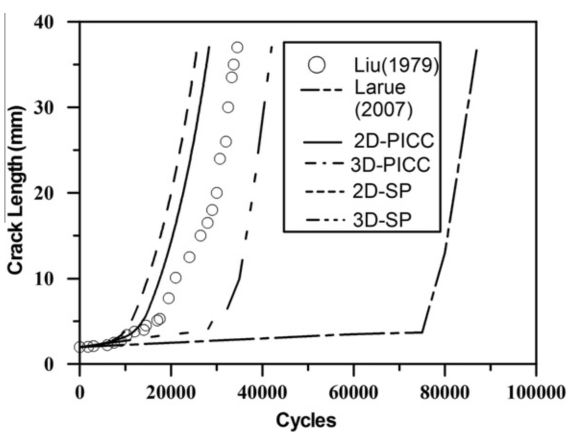

Fig. 11. Results of fatigue life predictions using 2D and 3D FEM simulation for A2-30 specimen, where SP stands for superposition technique.

prediction based on LaRue and Daniewicz (2007) work and the present 2D modeling is just 5%.

To clarify the discussion above the exact opening stress intensity factor (Ḱop) is assumed to be:

$$K'_{op} = \alpha K_{op} \tag{7}$$

where α is a correction factor and K_{op} is the opening stress intensity factor predicted by PICC. Fatigue life predictions based on different α values are shown in Fig. 12. It is clear that applying $\alpha = 1.05$ causes the fatigue life to differ by a factor of 1.2 and 1.16 for 2D and 3D FEM, respectively. In the case of $\alpha = 1.1$, the 2D and 3D predictions overestimate the fatigue life by factors of 1.31 and 1.2, respectively. Thus, the fatigue life prediction based on the crack closure method is highly sensitive to the opening stress intensity factor.

5.4. Comparison of PICC and superposition method

Fatigue crack growth was studied by Jones and Dunn (2009) based on the linear elastic fracture mechanics and the principle of superposition. The results were compared to the experimental data of Liu (1979). The results obtained in the present investigation (Fig. 11) that is based on the 2D and 3D PICC method show a better correlation to the Liu (1979) experimental data.

The observed difference between predicted fatigue lives of 2D and 3D analysis in Jones and Dunn (2009) investigation was attributed to the sensitivity of the fatigue life to the initial residual stresses. However, in the present PICC method the initial residual

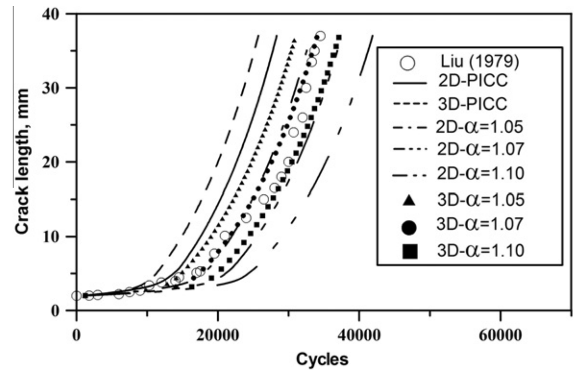

Fig. 12. Variation of crack length versus life cycles at different initial crack length (a_0).

stress did not affect the fatigue life predictions as severely as it was in Jones and Dunn (2009) superposition method (factor of 2). Consequently, it can be concluded that the "PICC method" is less sensitive to initial residual stress than the "superposition method".

The Jones and Dunn (2009) superposition method shows that changing the initial crack length from 2 to 2.83 mm results in decreasing the estimated fatigue life by a factor of 2.3. This highlights the sensitivity of the superposition fatigue life prediction method to the initial crack size. The same analysis was conducted in the present PICC investigation. The results obtained are shown in Fig 13. It can be observed that changing the initial crack size causes the predicted life to be reduced by a factor 1.3.

Considering the analogies presented above the following conclusion can be drawn. The superposition fatigue life prediction method is much more sensitive to initial residual stress and initial crack length than is the PICC method. Thus, the PICC method is more stable and liable for fatigue life prediction.

5.5. Modified PICC method

In the present study a modified PICC method is developed on the basis of "α" correction factor. The correction factor is used to decrease the PICC fatigue life prediction errors. Considering α we have:

$$\Delta K_{eff} = K_{max} - \alpha\ K_{op} \tag{8}$$

Replacing ΔK_{eff} in Eq. (5):

$$N_{ai-af} = \sum_{ai}^{af} \frac{a_i}{C(K_{max} - \alpha K_{opm})_i^m} \tag{9}$$

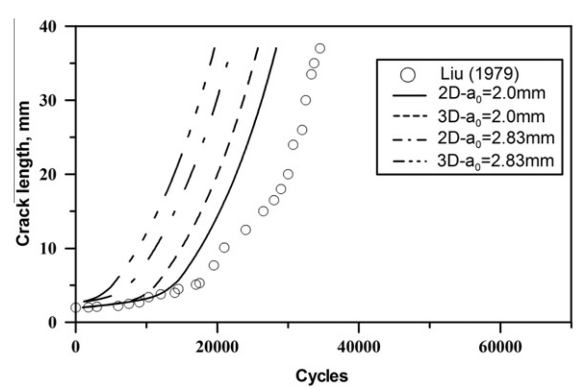

Fig. 13. Variation of crack length versus life cycles at different correction factors (α).

The alpha factor for 2D and 3D modeling is calculated on the basis of Liu's fatigue crack growth data (A2-30 specimen). The results of crack growth simulation were compared to Liu's experimental data and the alpha factor was set to minimize the fatigue life prediction errors (Fig. 12). Using Liu's data for A2-30 specimen and the procedure above the alpha factor was calculated as $\alpha_{3d} = 1.07$ and $\alpha_{2d} = 1.05$ for 3D and 2D modeling, respectively. Then, the crack growth relation was modified as:

$$N_{ai-af} = \sum_{ai}^{af} \frac{a_i}{C(K_{max} - 1.07\ K_{opm})_i^m} \quad \text{For 3D Modeling} \tag{10}$$

$$N_{ai-af} = \sum_{ai}^{af} \frac{a_i}{C(K_{max} - 1.05\ K_{opm})_i^m} \quad \text{For 2D Modeling} \tag{11}$$

Considering Eqs. (10) and (11), fatigue life predictions for 2D and 3D FEM are shown in Fig. 12. It is clear that the correction factors ($\alpha_{3d} = 1.07$ and $\alpha_{2d} = 1.05$) approximately reduces the 3D and 2D FEM error to zero and 5%, respectively.

6. Conclusions

Fatigue crack growth from a hole under the influence of residual stress field was predicted using 3D FEM and PICC method. The simulation results were compared to 2D FEM, superposition method and the experimental data of Liu. The following conclusions can be drawn from the analysis.

– The fatigue lives predicted by 3D elasto–plastic FEM and 2D plane stress FEM differed by a factor of 1.2.
– The PICC method is not as sensitive as the superposition method to initial residual stress distribution.
– Changing the initial crack size from 2 to 2.83 mm, caused the predicted fatigue life to be reduced by a factor of 1.3 and 2.3 in PICC and superposition method, respectively. Thus, the superposition fatigue life predictions are much more sensitive to initial crack length.
– PICC method of fatigue life prediction is highly sensitive to the opening stress intensity factor deviation.
– A new modified PICC method was established. Applying the correction factor ($\alpha = 1.07$) approximately reduces the 3D FEM errors to zero.

References

Castro, A., Potirniche, G.P., 2010. Multi-mechanism crack closure simulations in various steels. Int. J. Fatigue 32, 1764–1773.

Chermahini, R.G., Blom, A.F., 1991. Variation of crack-opening stresses in three-dimensions: finite thickness plate. Theor. Appl. Fract. Mech. 15, 267–276.

Chermahini, R.G., Blom, A.F., 1993. Fatigue crack growth and closure behavior of semicircular and semi-elliptical surface flaws. Int. J. Fatigue 16, 259–263.

De Matos, P.F., Nowel, D., 2007. On the accurate assessment of crack opening and closing stresses in plasticity-induced fatigue crack closure problems. Eng. Fract. Mech. 74, 1579–1601.

Dugdale, D.S., 1960. Yielding in steel sheets containing slits. J. Mech. Phys. Solids 8, 100–104.

Elber, W., 1970. Fatigue crack closure under cyclic tension. Eng. Fract. Mech. 2, 37–45.

Ismonov, S., Daniewicz, S.R., 2010. Simulation and comparison of several crack closure assessment methodologies using three-dimensional finite element analysis. Int. J. Fatigue 32, 1322–1329.

Jones, K.W., Dunn, M.L., 2009. Predicting fatigue crack growth from a preyielded hole. Int. J. Fatigue 31, 223–230.

LaRue, J.E., Daniewicz, S.R., 2007. Predicting the effect of residual stress on fatigue crack growth. Int. J. Fatigue 29, 508–515.

Liu, A.F., 1979. The effect of residual stresses on crack growth from a hole. NOR 79–74.

McClung, R.C., Sehitoglu, H., 1989. On the finite element analysis of fatigue crack closure-1, basic modeling issues. Eng. Fract. Mech. 33, 237–252.

Newman, J.C., 1981. A crack closure model for predicting fatigue crack growth under aircraft spectrum loading. In: Chang, J.B., Hudson, C.M. (Eds.), Methods and Models For Predicting Fatigue Crack Growth Under Random Loading, ASTM STP 748. American Society for Testing and Materials, Philadelphia, pp. 53–84.

Parker, A.P., 1982. Stress intensity factors, crack profiles, and fatigue crack growth rates in residual stress fields. In: Residual Stress Effects In Fatigue. ASTM STP 776. ASTM International, West Conshohocken, PA (pp. 224–234).

Seshadri, B.R., 1995. Numerical simulation and experimental correlation of crack closure phenomenon under cyclic loading. Ph.D. dissertation, Indian Institute of Science, Bangalore.

Sheu, B.C., Song, P.S., Hwang, S., 1995. Shaping exponent in wheeler model under a single overload. Eng. Fract. Mech. 51, 135–143.

Skinner, J.D., Daniewicz, S.R., 2001. Simulation of plasticity-induced fatigue crack closure in part-through cracked geometries using finite element analysis. Eng. Fract. Mech. 69, 1–11.

Solanki, K.N., 2002. Two- and three-dimensional finite element analysis of plasticity-induced crack closure – A comprehensive parametric study, MS thesis, Department of Mechanical Engineering, Mississippi State University.

Solanki, K., Daniewicz, S.R., Newman, S.J.C., 2004. Finite element analysis of plasticity-induced fatigue crack closure: an overview. Eng. Fract. Mech. 71, 149–171.

Zhang, J.Z., Bowen, P., 1998. On the finite element simulation of three-dimensional semi-circular fatigue crack growth and closure. Eng. Fract. Mech. 60, 341–360.